Local piezoelectric properties of ZnO thin films prepared by RF-plasma-assisted pulsed-laser deposition method

2010 Nanotechnology 21 235703

(http://iopscience.iop.org/0957-4484/21/23/235703)

Nanotechnology **21** (2010) 235703 (6pp) doi:10.1088/0957-4484/21/23/235703

Local piezoelectric properties of ZnO thin films prepared by RF-plasma-assisted pulsed-laser deposition method

I K Bdikin[1], J Gracio[1], R Ayouchi[2], R Schwarz[2] and A L Kholkin[3]

[1] Centre for Mechanical Technology and Automation, Universidade de Aveiro, 3810-193 Aveiro, Portugal
[2] Departamento de Fisica, Instituto Superior Técnico, 1049-001 Lisboa, Portugal
[3] Departamento de Engenharia Cerâmica e do Vidro and CICECO, Universidade de Aveiro, 3810-193 Aveiro, Portugal

E-mail: bdikin@ua.pt

Received 3 February 2010, in final form 7 April 2010
Published 13 May 2010
Online at stacks.iop.org/Nano/21/235703

Abstract

Zinc oxide (ZnO) thin films were grown on uncoated and zinc-coated Corning glass substrates by pulsed-laser deposition (PLD). X-ray diffraction measurements revealed that the as-deposited films are polycrystalline having preferential orientation along the [0002] and [10$\bar{1}$1] directions. Transmittance spectroscopy verified that the as-deposited films are transparent with a direct bandgap of about 3.28 eV at room temperature. Piezoresponse imaging and local hysteresis loop acquisition were performed to characterize the piezoelectric and possible ferroelectric properties of the films. The out-of-plane (effective longitudinal, $d_{\parallel}$) and in-plane (effective shear, $d_{\perp}$) coefficients were estimated from the local piezoresponse based on the comparison with $LiNbO_3$ single crystals. Measurements of all three components of piezoresponse (one longitudinal and two shear signals) allowed constructing piezoelectric maps for polycrystalline ZnO and to relate the variation of piezoelectric properties to the crystallographic and grain structure of the films. A shifted piezoresponse hysteresis loop under high voltages hints at the possible pseudoferroelectricity, as discussed recently by Tagantsev (2008 *Appl. Phys. Lett.* **93** 202905).

(Some figures in this article are in colour only in the electronic version)

1. Introduction

Zinc oxide (ZnO) is a well-known n-type semiconductor material having remarkable electronic and optical properties with great potential for micro- and optoelectronics [1–5]. Highly resistive *c*-axis-oriented ZnO films are also of interest for various piezoelectric applications (e.g. as sensors, actuators, high-frequency acoustic transducers, etc) due to their notable and stable piezoelectric properties [6]. Recently, ZnO has become a material of choice for piezoelectric harvesting devices because of the ease of growth in the nanorod and nanobelt geometries [7]. However, the piezoelectric properties of ZnO are not well characterized and understood, especially in the case of polycrystalline films having mixed orientation of the grains and weak (if any) unipolarity. These films are much easier to produce than their epitaxial counterparts but their piezoelectric properties should be understood and related to the microstructure, the degree of texture and growth conditions.

Piezoelectric properties of ZnO have been investigated by several authors [8–10]: however, the obtained data vary quite appreciably. The longitudinal piezoelectric coefficient (d_{33}) of undoped ZnO was found to range from 4.41 pm V^{-1} in nanorods [8] to 9.93 pm V^{-1} (single crystals) and reached the highest value of 26.7 pm V^{-1} in ZnO nanobelts [10]. Doping was found to have a pronounced effect on both microstructure and piezoelectric properties of ZnO. Piezoelectric properties were evaluated in ZnO films doped with Cu, Ni, Co and Fe and the longitudinal piezoelectric coefficients varied from 5 to 14 pm V^{-1} [11]. Further, the strong increase of d_{33} (up to 110 pm V^{-1}) was observed in V-doped ZnO films [12].

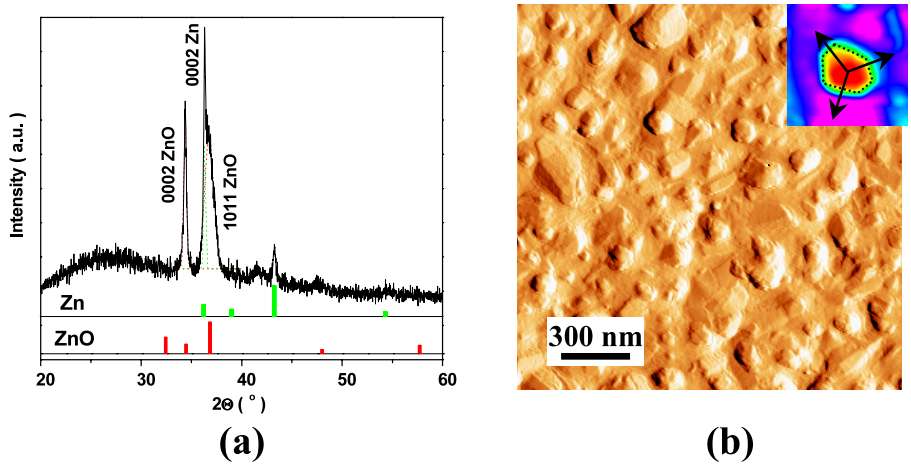

Figure 1. (a) X-ray diffraction spectra of textured ZnO films. Lines indicate ZnO and Zn peaks. (b) Topography (deflection) AFM image of the film's surface. The inset to (b) is a representative image of hexagonal grain.

In addition, ferroelectric properties were found in Li-, Mg- and V-doped films where piezoelectric hysteresis could also be observed. Piezoelectric properties of polycrystalline films having some degree of texture are obviously lower than in single crystals or epitaxial films and local piezoelectric measurements are thus necessary to relate the piezoresponse of individual grains to the macroscopic piezoactivity. A number of techniques have been used in the past to prepare ZnO thin films [13]. Among them, the pulsed-laser deposition (PLD) method is one of the best due to its simplicity combined with flexibility in the choice of processing parameters. However, the fundamental problem with the PLD technique, especially with ceramic targets, is the production of unwanted droplets and the reactivity of the atomic gases. To overcome this problem, metallic zinc targets are often used, and a radio-frequency (RF) generator is coupled to the ablation chamber in order to increase the density of ionized species, which can then be more easily incorporated into the growing film [13].

2. Experimental procedure

In this work, ZnO films were obtained using the RF-plasma-assisted PLD method. Details of the deposition system can be found elsewhere [14]. The deposition chamber has been initially evacuated down to 10^{-6} mbar, whereas the depositions were performed in a static O_2 plasma atmosphere (pressure 0.2 mbar). The ionized species were obtained using an RF generator (13.56 MHz, 3 W) connected to the target holder through an appropriate matching unit. The deposition time was typically 60 min. After the deposition process, the samples were allowed to cool down to room temperature in a pure oxygen atmosphere. The thickness of the films was about 200 nm. The films were deposited either onto bare 7059 Corning glass substrates or onto those with a prior-deposited Zn electrode.

To examine the structure and microstructure, x-ray diffraction (XRD) studies were carried out with a Rigaku diffractometer (Geigerflex D/Max, C Series, Tokyo, Japan) using Cu Kα radiation at 40 kV. Optical properties were evaluated on films grown on bare glass substrates. Transmission spectra were recorded in the range of 250–800 nm. A commercial AFM (NT-MDT, Ntegra Prima) was used for the local piezoelectric measurements in a piezoresponse mode [15]. The microscope was equipped with an external lock-in amplifier (SR-830, Stanford Research) and a function generator (FG120, Yokogawa), which were used to apply the ac and dc voltages to the film surface for poling, imaging and local piezoelectric hysteresis loop acquisition [16, 17]. The amplitude and frequency of the ac voltage were 1–5 V and 5 kHz, respectively. The dc voltage (up to 40 V) was stepped at a fixed position to acquire local hysteresis loops. Stiff conducting Si cantilevers (PPP-NCHR, Nanosensors) were used for these measurements to avoid electrostatic contributions. The details of the PFM measurements can be found elsewhere [16].

3. Results and discussion

Figure 1(a) shows the representative x-ray diffraction pattern of a ZnO thin film deposited at 400 °C, where only two strong peaks are observed in the 2θ range between 30° and 40°. The strongest peak consists of two superimposed peaks observed at $2\theta = 36.322°$ and 36.762°. They can be attributed to the (0002) plane of metallic Zn and the $(10\bar{1}1)$ plane of hexagonal ZnO, respectively. The second one, less intense, is observed at $2\theta = 34.38°$ and can be attributed to the (0002) plane of the hexagonal ZnO (JCPDS card 6-0416) having a wurtzite structure with $P6_3mc$ space group. As expected for the PLD method used, a Zn layer (electrode) grows preferentially along the c-axis orientation normal to the substrate. In contrast, ZnO films have been textured along the [0001] and $[10\bar{1}1]$ directions of the hexagonal lattice.

Figure 1(b) represents the surface topography of ZnO films obtained by AFM. The average RMS roughness was about 35 nm for the scan 1.5 × 1.5 μm^2. It is apparent that the film surface is relatively smooth without holes, cracks, protrusions or other defects, and consists of grains of two types: hexagonal ones (inset to figure 1(b)) with lateral dimensions of 50–100 nm and small grains (less than 50 nm

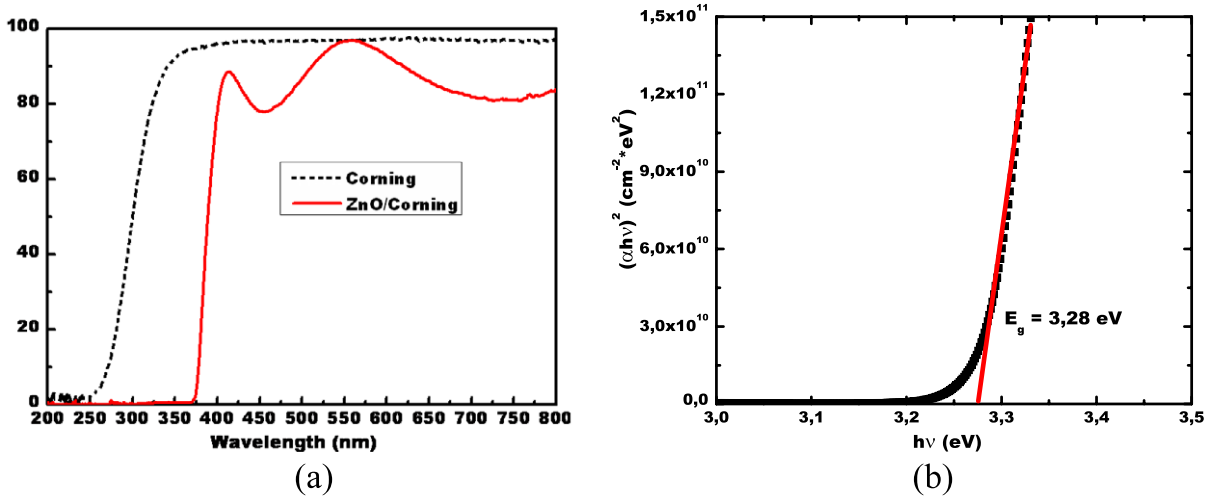

Figure 2. (a) Optical transmission spectra of a ZnO film on Corning glass substrate. (b) Variation of $(\alpha h\nu)^2$ versus $(h\nu)$ near the fundamental absorption edge.

in size) of a round shape. The appearance of these hexagonal grains and small grains are consistent with the XRD results predicting the coexistence of (0001) and $(10\bar{1}1)$ textures.

The films had good optical properties and were highly transparent in the visible range with an average transmittance reaching values up to 98%, and presented a sharp UV cutoff at ≈380 nm which corresponds to the fundamental band edge of undoped ZnO (figure 2(a)). From the optical absorption spectrum the optical energy bandgap (E_g) is estimated to be 3.28 eV (figure 2(b)). This value is close to the reported values of 3.2–3.3 eV for intrinsic undoped ZnO at room temperature [18].

XRD measurements (figure 1(a)) indicate that there are two main orientations of the grains, i.e. coexistence of grains with (0001) and $(10\bar{1}1)$ texture. These types of textures are characteristic for ZnO [19]. In principle (for electroded unclamped grains), the measured piezoresponse should be determined by the relevant piezoelectric coefficient (d_{33}, d_{31} and d_{15}) and by the orientation of the individual grains relative to the substrate plane. For *c*-oriented grains the piezoelectric strain ε is simply related to the longitudinal (d_{33} coefficient) and differs by the phase (0° or 180° between the applied field and the measured displacement): $\varepsilon_3 = d_{33}E_3$ for (0001) grain and $-\varepsilon_3 = d_{33}$ $(-E_3)$ for $(000\bar{1})$ grain. Zero of the phase corresponds to 'positive' orientation of the grains and positive piezoresponse signal when the electrical field is positive. The 180° of the phase corresponds to a 'negative' orientation of the grains. For $(10\bar{1}1)$-oriented grains the situation is more complicated and the effective piezoelectric coefficient is determined by the rotation of the piezoelectric matrix around some angle α (figure 3(g)):

$$d_{ijk} = A_i^m A_j^n A_k^l d_{mnl}^o, \tag{1}$$

where d_{ijk} and d_{mnl}^o are the rotated and initial tensors, respectively, and A_i^j is the transformation matrix. For the case of hexagonal symmetry equation (1) is reduced to simple expressions for the effective longitudinal and transverse coefficients, $d_\parallel$ and $d_\perp$, in an arbitrary direction described by the angle α:

$$\begin{aligned} d_\parallel &= (d_{31} + d_{15})\sin^2\alpha\cos\alpha + d_{33}\cos^3\alpha \\ d_\perp &= [d_{31} - d_{33} + (d_{15} + d_{31} - d_{33})\cos 2\alpha]\sin\alpha. \end{aligned} \tag{2}$$

The effective piezoelectric response measured by PFM is thus a combination of all three independent piezoelectric coefficients and can be calculated for the given texture based on the tabulated values for ZnO single crystals [20] and the angle estimated for $(10\bar{1}1)$ orientation. The results are shown in table 1. The value of $d_\parallel$ for tilted grain was also normalized to the value of the piezocoefficient for the (0001) grain. It follows from equations (2) that the small variations in d_{33}, d_{31} and d_{15} could result in a strong variation in both $d_\parallel$ and $d_\perp$. Thus the calculated values could be a rough approximation to the local piezoproperties. It should be noted that, for the present ZnO texture, we expect four different levels of the out-of-plane contrast (OOP) corresponding to 'positive' and 'negative' (0001 and $10\bar{1}1$) grains. The ratio between 'positive' and 'negative' grains is a measure of the unipolarity of the films, and thus of the macroscopic piezoelectric response useful for various piezoelectric applications.

Figure 3 shows the topography and corresponding $d_\parallel$ and $d_\perp$ (for two orthogonal components related to the scanning directions) piezoelectric contrasts. Two different IP (in-plane, I_{IPx} and I_{IPy}) images with sample rotation at 90° around the normal to the surface provide two components $d_{\perp x}$ and $d_{\perp y}$ (figures 3(c) and (d)). To determine the absolute value of the effective shear (in-plane) response we used a simple expression for the IP signal proportional to $d_\perp$: $\mathrm{IP} = \sqrt{\mathrm{IP}_x^2 + \mathrm{IP}_y^2}$. In addition, the cross sections of the corresponding signals (figure 3(f)) demonstrate a correlation between OOP and IP signals for grains on the images in figures 3(b)–(d). The OOP maximum corresponds to a minimum of the IP signal and for the IP maximum the OOP signal has an intermediate level corresponding to the $(10\bar{1}1)$ grain (figure 3(f)). Figure 3(e)

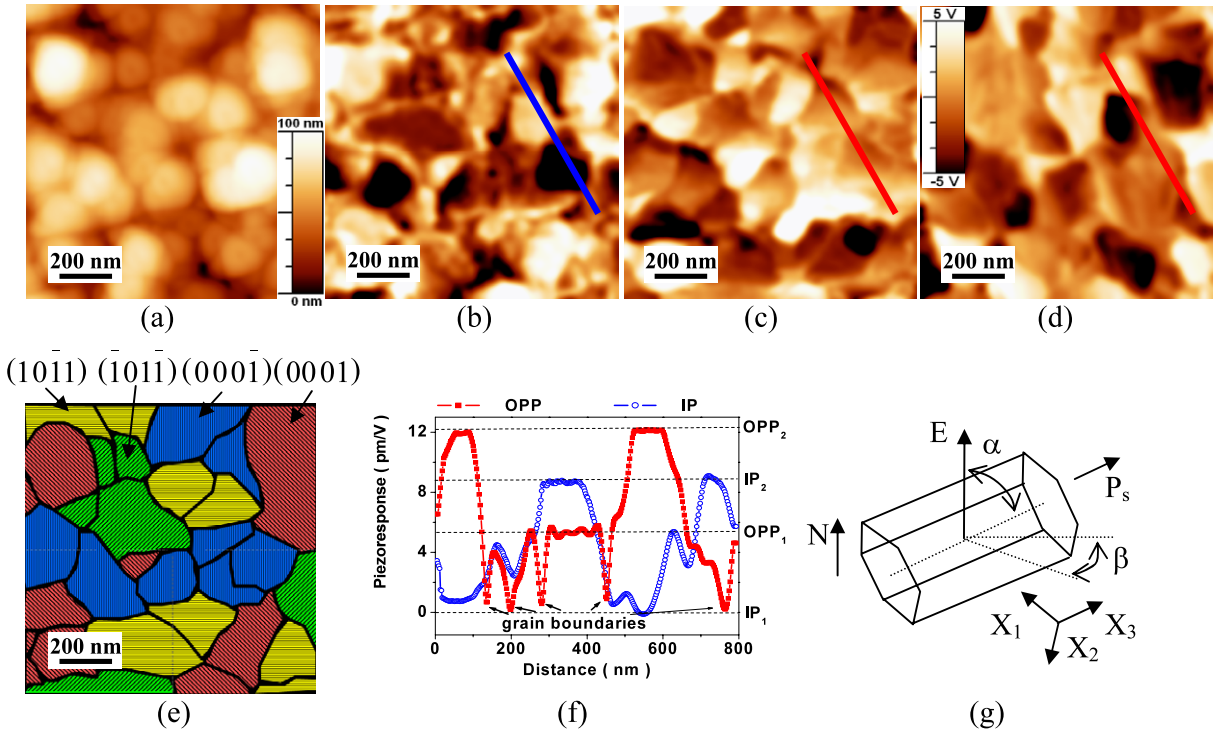

Figure 3. Topography (a), OPP (b), IP (c) and (d) piezoresponse images of the ZnO film on the same area, with $V_{ac} = 2.5$ V and $f = 5$ kHz. (e) Distribution of 'positive' and 'negative' ZnO grains reconstructed by comparison of OPP and IP signals. (f) Cross sections of IP and OPP images. (g) Schematic illustration of the (10$\bar{1}$1)-oriented ZnO grain. N—normal to sample surface, E—electric field, P_s—polarization of ZnO grain, α—angle between P_s and E, β—angle of orientation of the ZnO grain around N.

Table 1. Effective piezoelectric coefficients of ZnO films based on calculations via equations (2) and our data.

Piezoelectric coefficients	$d_{\parallel}$ (0001) (pm V^{-1})	$d_{\parallel}$ (10$\bar{1}$1) (pm V^{-1})	$d_{\parallel}$ (10$\bar{1}$1)/$d_{\parallel}$ (0001)	$d_{\perp}$ (10$\bar{1}$1) (pm V^{-1})
Calculated based on equations (2)	12.4	6.2	0.50	2.7
Our data	12.0	5.3	0.44	8.2

shows the real distribution of 'positive' and 'negative' grains reconstructed by comparison of OPP and IP signals.

As already mentioned, the $d_{\parallel}$ contrast should contain four different signal levels corresponding to 'positive' and 'negative' grains of both orientations. The ratio between the amplitudes of the out-of-plane signals could be evaluated and compared with the calculated value (table 1). This was indeed observed in the films (figure 3) and the corresponding cross sections of the amplitudes (figures 3–(d)) provide the ratio between piezoelectric amplitudes for (0001) and (10$\bar{1}$1) grains (0.44±0.02). This value is close to the theoretical one (table 1) and thus validates our rough approximation which does not take into account apparent clamping of the grains [21].

Based on the measured PFM signals we could estimate piezoelectric coefficients for our ZnO films using a simple calibration with $LiNbO_3$ single crystals (LNO) [22]. The $LiNbO_3$ calibration sample with the appropriate orientation was first measured by the PFM and the amplitude of both out-of-plane and in-plane signals were recorded at the chosen frequency and ac voltage level. The LNO sample was then replaced with the ZnO film using the same settings of the PFM and laser system alignment and the amplitudes of the corresponding signal in ZnO were directly compared with those of LNO samples with known piezoelectric coefficients [23]. As the dielectric constant anisotropy is not very different in both materials we believe this method gives a reasonable evaluation of the bulk piezoelectric coefficients $d_{\parallel}$ and $d_{\perp}$ (rather than their local analogs). The histograms of the OOP and IP PFM signals from the image in figure 3 are shown in figure 4. The histogram of the OOP image consists of two maxima with $d_{\parallel} \approx 12$ and ≈5.3 pm V^{-1}. The histogram of the IP signal (figure 4(b)) also reveals two peaks: one at the zero position (corresponding to the noise) and another at ≈8.2 pm V^{-1}. These were compared with the calculated values (table 1). Good correspondence of the experimental and calculated values was observed only for the vertical (OOP) response. The measured lateral (shear) piezoelectric coefficient is several times greater than the calculated value. This difference cannot be attributed to clamping (which usually reduces the effective piezocoefficient) and can be attributed to the specific microstructure of the films [24] and possible dependence of effective $d_{\perp}$ on the grain morphology.

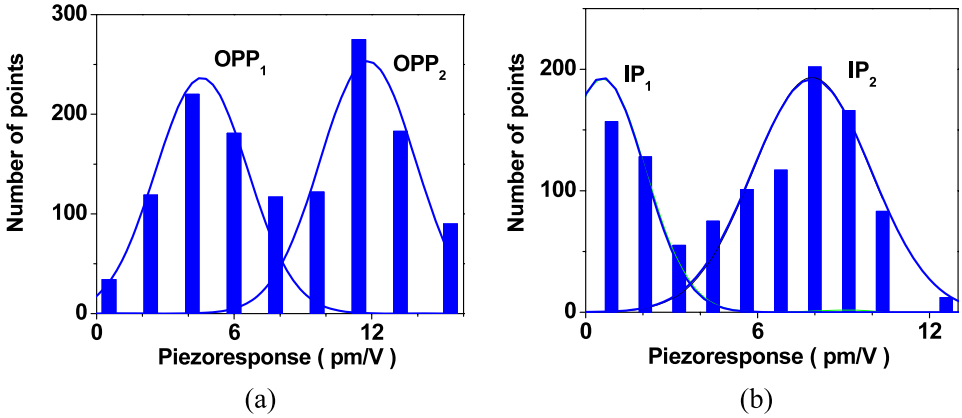

Figure 4. Histograms of the PFM images of the ZnO. (a) OPP image and (b) IP image.

Table 2. Relative areas of (0001) and $(10\bar{1}1)$ grains with 'positive' and 'negative' polarizations.

	Orientation	
Polarization	(0001)	$(10\bar{1}1)$
'Positive' grains	26.7%	19.6%
'Negative' grains	21.9%	14.0%

It is interesting to calculate unipolarity of the ZnO films based on their local response (in both types of grains) and compare it with the macroscopic properties. In terms of local piezoelectric activity, the unipolarity (UP) of the columnar film can be written as

$$\mathrm{UP} = \frac{(\sum_i S_i^+ - \sum_j S_j^-)k_{0001} + (\sum_l S_l^+ - \sum_m S_m^-)k_{10\bar{1}1}}{\sum_{n=1}^{N} S_n k_n} \tag{3}$$

where S^+ and S^- are the areas occupied by the 'positive' and 'negative' grains for both orientations, k_{0001} and $k_{10\bar{1}1}$ are piezoresponse signals for (0001)-and $(10\bar{1}1)$-oriented grains, and N is the total number of grains in the analyzed image. The results averaged from several scans are shown in table 2. It is seen that, for the (0001) grains, there is a prevalence of the 'positive' grains in proportion of approximately 1.2, i.e. 'positive' grains (with the polar vector directed towards the free surface of the film) dominate the piezoelectric response. $(10\bar{1}1)$ grains represent the same trend but with a prevalence factor of about 1.4. The total unipolarity of the film calculated based on the weight factor, taking into account the piezoelectric activity of both grains, is about 11%. It means, on average, the piezoelectric activity of the films is about nine times weaker compared to the case of 100% polar axis alignment in one direction. This is related to the nucleation stage of the films' growth where arriving species may accommodate themselves on the bottom electrode either with oxygen or zinc planes and corresponding polar vector. It is clear that the unipolarity (along with the texture) is the most important parameter that should be maximized by varying the processing conditions during film growth. This study is currently ongoing and will be published elsewhere. It should only be mentioned here that polycrystalline textured ZnO films can

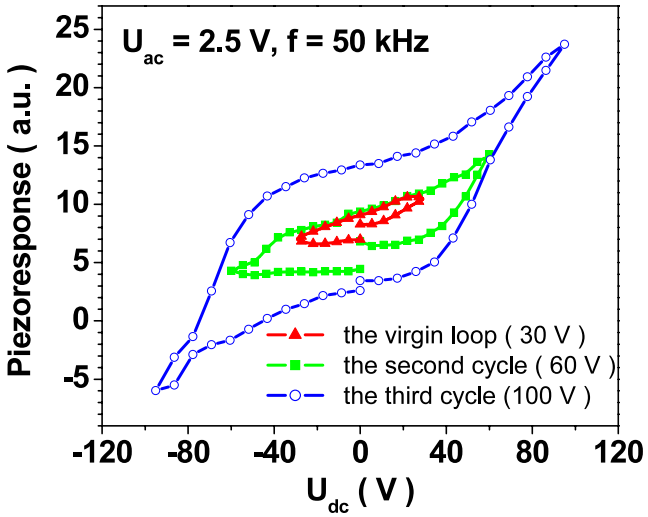

Figure 5. Local piezoresponse hysteresis loop of the ZnO.

be good candidates for piezoelectric applications provided their unipolarity approaches 100%. PFM measurements are indeed indispensable to relate the crystallographic texture and microstructure to the local, and finally to the macroscopic, response. The representative polarity map of the studied ZnO films (figure 3(e)) illustrates the conclusion given above.

Finally, the weak hysteresis of the OOP signal was observed under varying dc field. The observed hysteresis could be a consequence of the pseudoferroelectricity in ZnO films as recently discussed by Tagantsev [25]. His theoretical considerations predict that the ferroelectric behavior is due to the weak internal field that reduces the symmetry of the crystal above the phase transition and allows solving the problem of the symmetry incompatibility in ZnO. In this case, a broad maximum of the dielectric constant and the shift of the phase transition is related to crossing the Widom line. The results shown in figure 5 are compatible with this scenario, displaying a strong imprint and weak internal bias field (shift of the hysteresis loop in one direction). The coercive field at room temperature is so high that the film cannot be fully switched before breakdown [26] and may actually describe a well-known partial loop [27]. The sharp and linear tips of the loop

could be related to the degradation caused by the increasing conductivity and are not related to the ferroelectric behavior. It should be mentioned that the observed hysteresis is sensitive to the chosen location and is perhaps related to the impurities and defects as was initially discussed in the case of doped ZnO [28].

4. Conclusions

In conclusion, we determined the distributions of both out-of-plane and in-plane piezoresponse signals in textured ZnO thin films via three-dimensional piezoresponse force microscopy [29, 30]. Both signals are compatible with the crystallographic texture of the films and provide unipolarity and maps of the piezoelectric coefficients for polycrystalline ZnO. The measured longitudinal piezocoefficients are close to those calculated based on single-crystal values and the specific texture of the films. Using the piezoelectric maps we could predict the unipolarity of the films, which is the most important factor for their piezoelectric applications. It is shown that the unipolarity is sufficiently small for both types of grains, giving an average value of about 11%. Hysteresis-like behavior of the out-of-plane signal suggests pseudoferroelectricity in undoped ZnO with the coercive field above the breakdown field in this material.

Acknowledgment

RA is grateful for getting funds from the Foundation of Science and Technology (FCT), Portugal (grant no. SFRH/BPD/34111/2006).

References

[1] Wang Z L 2004 *J. Phys.: Condens. Matter* **16** R829
[2] Fonoberov V A and Balandin A A 2006 *J. Nanoelectron. Optoelectron.* **1** 19
[3] Kalinina E V, Cherenkov A E, Onushkin G A, Alivov Y I, Look D C, Ataev B M, Oamev A K and Chukichev C M 2005 *Zinc oxide—a Material for Micro- and Optoelectronic Applications* ed N K Nickel and E Terukov (Dordrecht: Springer) p 211
[4] Wang X, Summers C J and Wang Z L 2004 *Nano Lett.* **4** 423
[5] Özgür Ü, Alivov Ya I, Liu C, Teke A, Reshchikov M A, Doğan S, Avrutin V, Cho S-J and Morkoç H 2005 *J. Appl. Phys.* **98** 041301
[6] Hickermell F S 1976 *Proc. IEEE* **64** 631
[7] Wang Z L 2007 *Mater. Today* **10** 20
[8] Scrymgeour D A, Sounart T L, Simmons N C and Hsu J W P 2007 *J. Appl. Phys.* **101** 014316
[9] Xiang H J, Yang J, Hou J G and Zhu Q 2006 *Appl. Phys. Lett.* **89** 223111
[10] Zhao M H, Wang Z L and Mao S X 2004 *Nano Lett.* **4** 587
[11] Wang X B, Song C, Li D M, Geng K W, Zeng F and Pan F 2006 *Appl. Surf. Sci.* **253** 1639
[12] Yang Y C, Song C, Wang X H, Zeng F and Pan F 2008 *Appl. Phys. Lett.* **92** 012907
[13] Cracium F, Dinescu M, Verardi P, Scaresorianu N, Galassi C and Piazza D 2004 *Ferroelectrics* **302** 313
[14] Sanguino P, Koynov S, Niehus M, Melo L, Schwarz R, Alves H and Meyer B K 2001 *Mater. Res. Soc. Symp. Proc.* **693** 81
[15] Kalinin S V, Setter N and Kholkin A L (ed) 2009 Electromechanics on the nanometer scale: emerging phenomena, devices, and applications *Mater. Res. Soc. Bull.* **34** 634
[16] Jesse S, Lee H and Kalinin S V 2006 *Rev. Sci. Instrum.* **77** 073702
[17] Kholkin A L, Kalinin S V, Roelofs A and Gruverman A 2006 *Scanning Probe Microscopy: Electrical and Electromechanical Phenomena at the Nanoscale* vol 1, ed S Kalinin and A Gruverman (Berlin: Springer)
[18] Srikant V and Clarke D R 1998 *J. Appl. Phys.* **83** 5447
[19] Yan X, Li Zh, Zou Ch, Li S, Yang J, Chen R, Han J and Gao W 2010 *J. Phys. Chem.* C **114** 1436
[20] Crisler D F, Cupal J J and Moore A B 1968 *Proc. IEEE* **56** 225
[21] Royer D and Kmetik V 1992 *Electron. Lett.* **28** 1828
[22] Kholkin A, Amdursky N, Bdikin I, Gazit E and Rosenman G 2010 *ACS Nano* **4** 610
[23] Landolt H and Bornstein R 1981 *Numerical Data and Functional Relationships in Science and Technology* (*New Series* vol III/16) (Berlin: Springer)
[24] Nagarajan V, Jenkins I G, Alpay S P, Li H, Aggarwal S, Salamanca-Riba L, Roytburd A L and Ramesh R 1999 *J. Appl. Phys.* **86** 595
[25] Tagantsev A 2008 *Appl. Phys. Lett.* **93** 202905
[26] Gupta V and Mansingh A 1998 *ISAF XI'98: Proc. XI IEEE Symp. on Applications of Ferroelectrics (Montreux, Aug. 1998)* p 113
[27] Damjanovic D 2005 *Science of Hysteresis* vol III, ed G Bertotti and I Mayergoyz (Amsterdam: Elsevier) chapter 4 (Hysteresis in Piezoelectric and Ferroelectric Materials) pp 337–465
[28] Pearton S J, Norton D P, Ip K, Heo Y W and Steiner T 2005 *Prog. Mater. Sci.* **50** 293
[29] Eng L M, Güntherodt H-J, Schneider G A, Kopke U and Saldaña J M 1999 *Appl. Phys. Lett.* **74** 233
[30] Kalinin S V, Rodriguez B J, Jesse S, Shin J, Baddorf A P, Gupta P, Jain H, Williams D B and Gruverman A 2006 *Microsc. Microanal.* **12** 1